Journal of Nano Research
ISSN: 1661-9897, Vol. 85, pp 37-42
doi:10.4028/p-00NxeD

Submitted: 2023-11-14
Revised: 2024-05-15
Accepted: 2024-07-12
Online: 2024-11-29

Phase-Field Approach to Formation of Aluminum Oxyhydroxide Nanofibrils on a Liquid Aluminum Alloy Surface in Water-Containing Atmospheres

MICHAEL Sorokin[1,a*], ANATOLE Khodan[2,b],
ISHAQ Ahmad[3,c], NAVEED Zafar Ali[3,d] and SHEHLA Honey[4 e]

[1]National Research Centre ‘Kurchatov Institute’, Kurchatov Square 1, 123182 Moscow, Russia

[2]A.N. Frumkin Institute of Physical Chemistry and Electrochemistry RAS,
Leninskiy Prospekt, 31/4, 119071 Moscow, Russia

[3]National Centre for Physics, Islamabad 44000, Pakistan

[4]University of Okara, 2 KM Multan Road Renala Khurd By Pass, 56300 Okara, Pakistan

[a]m40@lab2.ru , [b]anatole.khodan@gmail.com, [c]ishaq.ahmad@ncp.edu.pk, [d]nzafar@ncp.edu.pk,
[e]shehlahoney@yahoo.com

Keywords: aluminum amalgam; aluminum oxidation; aluminum oxyhydroxide nanofibrils; phase-field modelling.

Abstract. Formation of peculiar nanofibril structures on the surface of liquid aluminum alloys as a result of chemical reaction of aluminum with water vapors was well studied experimentally for various alloy components starting from mercury. However, the mechanism of nanofibril formation remains unclear to date, and the lack of an appropriate theoretical model does not allow evaluation of the structure parameters depending on the process conditions.

We assume that the interface layer between the liquid metal phase and the atmosphere, containing the water vapor, develops certain inhomogeneities respect to the content of hydroxyl groups. That provides areas of suppressed and enhanced diffusion of the aluminum from the liquid phase toward the atmosphere contact. Phase-field modeling, taking into account their elastic interaction, demonstrates formation of the array of nano-islands, enriched with hydroxyl groups, which can be precursors for formation and growth of nanofibrils with elements of pre-boehmite structure.

Introduction

Chemical reactions of water vapor with the surface of liquid aluminum alloys have been known for a long time starting from with the use of mercury [1]

$$2\ \mathrm{Al{\cdot}Hg} + 6\ \mathrm{H_2O} \rightarrow 2\ \mathrm{Al(OH)_3} + 2\ \mathrm{Hg} + 3\ \mathrm{H_2}\uparrow. \tag{1}$$

Aluminum hydroxide, creating in the exothermic reaction (1), forms a peculiar array of fibrils, growing on the reaction surface. The process was reproduced from amateur laboratories to industrial production and thoroughly studied experimentally [2-4]. It was found that various alloy components change the reaction temperature according to the alloy melting points from the ambient conditions for mercury up to 680 °C for pure aluminum, and the product corresponds to the stable form of the aluminum oxyhydroxide at the given temperature. As the alloy components besides the aluminum do not expend and can be reused, such reactions are also considered as hydrogen sources for green energy [5]. These investigations confirmed that the liquid alloy phase is important to avoid the hydrogen blistering and reaction freezing. From the other hand, for high relative humidity, in the utmost case of water condensation (or the sample immersion), the reaction does take place at the whole surface and provides flakes or gel-like clots rather than fibrils of the oxyhydroxide [6,7].

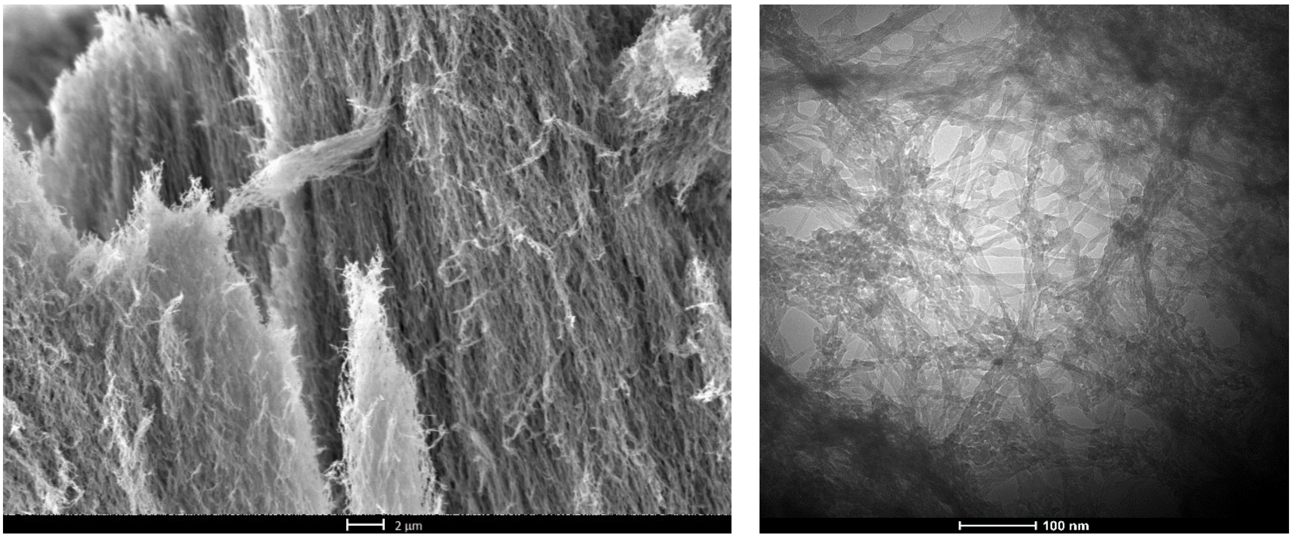

Fig. 1 SEM images of the aluminum oxyhydroxide structures formed on amalgam at 25º C and 70% relative humidity

Optimal relative humidity of 60-75% provides steady growth of amorphous $Al_2O_3{\cdot}nH_2O$ nanofibrils with n of 3.9 ÷ 4.2 on the amalgam surface (Fig. 1). Diameter of the single fibril is 5 ÷ 9 nm, and interestingly remains about the same for other alloys [4]. However, despite many advances in experimental studies of the nanofibrils formation and 1D growth, a lack of theoretical understanding of the process hinders its further research and application possibilities [4].

It seems reasonable to concentrate on the modelling of the initial stage of the fibril growth, which is crucial for the further structure parameters. We assume that the interface layer between the liquid metal phase and the atmosphere, containing the water vapor, develops certain inhomogeneities respect to the content of hydroxyl groups. That leads to the appearance of areas of enhanced (enriched with hydroxyl groups) and suppressed diffusion of the aluminum from the liquid phase toward the atmosphere contact. The latter then become the grow sites for nanofibrils. Phase-field modeling will be applied for the interface layer to check this assumption.

Phase-Field Model

Reaction (1), starting at the interface of the liquid aluminum amalgam and water-containing atmosphere, can continue as the forming aluminum oxyhydroxide islands are relatively permeable for aluminum and water. Moreover, these islands remain on the surface of liquid metal, dislike the similar reaction with solid aluminum, when the oxyhydroxide layer grows by penetration within the bulk, when the reaction gradually slows down and practically stops [7]. Thus, releasing mercury during the reaction (1) constantly provides liquid layer of the amalgam beneath the reaction interface.

In the case of 60-75% relative humidity, found to be optimal for fibril growth at room temperature, we suppose partial hydration of the surface layer. However, uniform distribution of the hydroxyl groups would be thermodynamically unfavorable, as there are stable stoichiometric compounds of aluminum oxide and oxyhydroxide. So, one can expect decay of the uniformly hydrated layer, and we employ the phase-field approach to model the process, assuming the forming nano-islands as the precursors of the further fibril growth (Fig. 2).

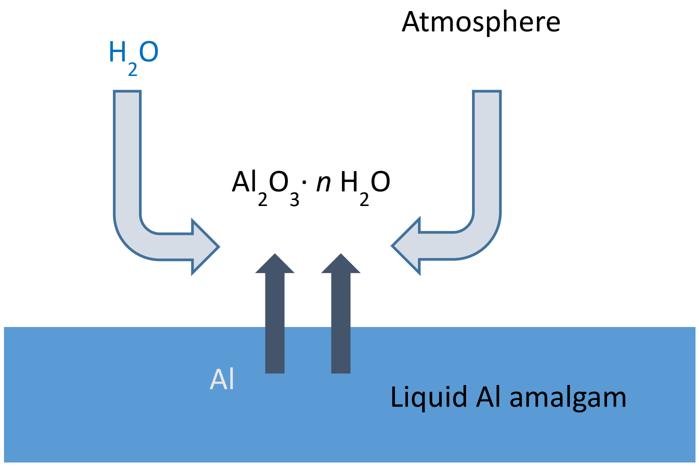

Fig. 2 Supposed mechanism of the aluminum oxide layer hydration and fibril growth

Total free energy of the surface layer, to be minimized in the framework of the phase-field approach depends on the surface concentration of the hydroxyl groups $c(\vec{r})$ through the chemical f and elastic e contributions, and the excess energy of interphase edges with the gradient coefficient κ.

$$\mathcal{F} = \int (f + e + \kappa(\nabla c)^2) d\vec{r} \tag{2}$$

Assuming the steady-state balance of the water adsorption, the concentration can be considered as a conservative order parameter, and the Cahn-Hilliard equation should be solved to find the concentration field evolution:

$$\frac{\partial c}{\partial t} = M\left(\nabla^2 \frac{\partial(f+e)}{\partial c} - 2\kappa\nabla^4 c\right) \tag{3}$$

Fourier transform can be employed for coordinate dependence that gives

$$c(\vec{r},t) \to \hat{c}(\vec{k},t)\ ,\quad \frac{\partial}{\partial x} \to ik_x\ ,\quad \frac{\partial}{\partial y} \to ik_y \tag{4}$$

and reduces the partial differential (Eq. 3) to ordinary differential equation for $\hat{c}(\vec{k},t)$, which can be solved using a finite difference scheme. However, the non-linear term in the (Eq. 3) should be recalculated for each time step [8].

Elastic energy: Elastic contribution $e(\vec{r})$ to the free energy density should be found from the elastic problem for a given transformation strain ε_{ij}^T, which assuming the Vegard's law [9], depending on the hydroxyl concentration $c(\vec{r})$:

$$\varepsilon_{ij}^T(\vec{r}) = \frac{c(\vec{r})}{a}\frac{\partial a}{\partial c}\delta_{ij} \tag{5}$$

The elastic strain is the difference between total strain u_{ij} and the transformation strain

$$\varepsilon_{ij} = u_{ij} - \varepsilon_{ij}^T\ , \tag{6}$$

where the total strain is determined by the displacement vector $\vec{u}$

$$u_{ij} = \frac{1}{2}\left(\frac{\partial u_i}{\partial x_j} + \frac{\partial u_j}{\partial x_i}\right). \tag{7}$$

Hooke's law connects the elastic strain with the stress tensor

$$\sigma_{ij} = C_{ijkl}\varepsilon_{kl} \tag{8}$$

Where the 4-rank stiffness tensor C_{ijkl} for an isotropic media reduces to two independent constants, e.g. Young's modulus E and Poisson ratio ν. Under plane stress conditions the Hooke's law reads

$$\sigma_{xx} = \frac{E}{1-\nu^2}\left(\varepsilon_{xx} + \nu\varepsilon_{yy}\right), \tag{9}$$

$$\sigma_{yy} = \frac{E}{1-\nu^2}\left(\nu\varepsilon_{xx} + \varepsilon_{yy}\right), \tag{10}$$

$$\sigma_{xy} = \frac{E\nu}{1+\nu}\varepsilon_{xy}. \tag{11}$$

Substituting (Eq. 5, 6) and (Eq. 9-11) to the mechanical equilibrium conditions

$$\frac{\partial \sigma_{ij}}{\partial x_j} = 0 \tag{12}$$

in two-dimensional isotropic case one obtains

$$\frac{\partial u_{xx}}{\partial x} + \nu\frac{\partial u_{yy}}{\partial x} + (1-\nu)\frac{\partial u_{xy}}{\partial y} = (1+\nu)\frac{1}{a}\frac{\partial a}{\partial c}\frac{\partial c}{\partial x}, \tag{13}$$

$$(1-\nu)\frac{\partial u_{xy}}{\partial x} + \nu\frac{\partial u_{xx}}{\partial y} + \frac{\partial u_{yy}}{\partial y} = (1+\nu)\frac{1}{a}\frac{\partial a}{\partial c}\frac{\partial c}{\partial y}, \tag{14}$$

that with account of the (Eq. 7) provides a closed system of second-order partial differential equations for the displacement vector components u_x and u_y. In the Fourier space it becomes a system of algebraic equations:

$$\left(k_x^2 + \frac{1-\nu}{2}k_y^2\right)\hat{u}_x + \frac{1+\nu}{2}k_x k_y \hat{u}_y = -ik_x\hat{c}(1+\nu)\frac{1}{a}\frac{\partial a}{\partial c}, \tag{15}$$

$$\frac{1+\nu}{2}k_x k_y \hat{u}_x + \left(k_y^2 + \frac{1-\nu}{2}k_x^2\right)\hat{u}_y = -ik_y\hat{c}(1+\nu)\frac{1}{a}\frac{\partial a}{\partial c}. \tag{16}$$

The point $k_x = k_y = 0$ corresponds to the average

Finally, the elastic energy contribution to the free energy [10]

$$e = \frac{1}{2}C_{ijkl}\varepsilon_{ij}\varepsilon_{kl} = \frac{E}{2(1+\nu)}\left(\varepsilon_{ij}^2 + \frac{\nu}{1-2\nu}\varepsilon_{ll}^2\right) \tag{17}$$

can be found, using (Eq. 6,7) and substituted into the Cahn-Hilliard (Eq. 3).

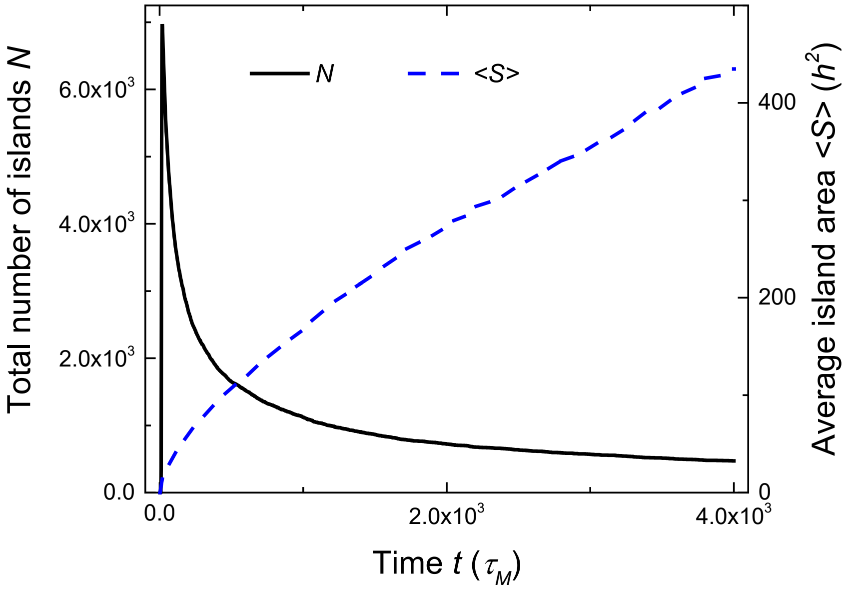

Fig. 3 Time evolution of the total number of islands and their average area for the given average hydroxyl group surface concentration $\langle c(\vec{r})\rangle = 0.25$

Results and Conclusions

Cluster analysis of the concentration field $c(\vec{r})$ demonstrates formation and evolution of the ensemble of nano-islands, enriched with the hydroxyl group (Fig. 3) [8].

Note, that initially arisen islands undergo the Ostwald ripening, which rapidly decreases their number. However, the further redistribution of the hydroxyl group within the interface layer slows down due to elastic interaction of the growing islands [11, 12]. The later effect should also push up the oxyhydroxide Island, forming a new fibril layer according to the (Fig. 2), and allowing the interface to absorb new hydroxyl groups, but this process is beyond the present consideration.

Thus, we propose a new model of the nanofibril structure formation, which is basically concordant with all known experimental findings. Phase-field approach was applied to support the model and develop a basis for further quantitative investigation and prediction of structures' parameters.

Acknowledgments

This work has been carried out using computing resources of the federal collective usage center Complex for Simulation and Data Processing for Mega-science Facilities at NRC "Kurchatov Institute", http://ckp.nrcki.ru/ .

Some of the experimental results were obtained within the framework of the program funded by the Russian Science Foundation: 22-23-01011 "New Composite Materials and Protective Coatings Based on 3D Porous Corundum Structures Filled with Tungsten or Tungsten Carbides Possessing Elevated Resistance in Gas and Plasma Flows with High Energy".

References

[1] H. Wislicenus, Über die faserähnliche gewachsene Tonerde (Fasertonerde) und ihre Oberflächenwirkungen (Adsorption), Zeitschrift für Chemie und Industrie der Kolloide 2 (1908) 11-20.

[2] Information on https://youtu.be/IrdYueB9pY4 .

[3] A. Khodan, A. Kanaev, M. Esaulkov, M. Kiselev, V. Nadtochenko, Effects of Surface Chemical Modification by Ethoxysilanes on the Evolution of 3D Structure and Composition of Porous Monoliths Consisting of Alumina Hydroxide Nanofibrils in the Temperature Range 25–1700 °C, Nanomaterials 12 (2022) 3591.

[4] A. Khodan, T.H.N. Nguyen, M. Esaulkov, M.R. Kiselev, M. Amamra, J.-L. Vignes, A. Kanaev, Porous monoliths consisting of aluminum oxyhydroxide nanofibrils: 3D structure, chemical composition, and phase transformations in the temperature range 25 – 1700 °C, J Nanopart Res 20 (2018) 194-204.

[5] S. Xu, X. Zhao, J. Liu, Liquid metal activated aluminum-water reaction for direct hydrogen generation at room temperature, Renewable and Sustainable Energy Reviews 92 (2018) 17-37.

[6] A.S. Lozhkomoev, E.A. Glazkova, N.V. Svarovskaya, O.V. Bakina, S.O. Kazantsev, M.I. Lerner, Specific features of aluminum nanoparticle water and wet air oxidation, AIP Conference Proceedings 1683 (2015) 020128.

[7] B.C. Bunker, G.C. Nelson, K.R. Zavadil, J.C. Barbour, F.D. Wall, J.P. Sullivan, C.F. Windisch Jr., M.H. Engelhardt, D.R. Baer, Hydration of Passive Oxide Films on Aluminum, J. Phys. Chem. B 106 (2002) 4705-4713.

[8] M.V. Sorokin, I. Ahmad, A.N. Khodan, S.O. Aisida, Pulsed laser deposition of epitaxial films: phase-field description. 2022 19th International Bhurban Conference on Applied Sciences and Technology (IBCAST), 2022, 10-13, doi: 10.1109/IBCAST54850.2022.9990074.

[9] L. Q. Chen, Phase-field models for microstructure evolution, Annu. Rev. Mater. Res. 32 (2002) 113-140.

[10] A.G. Khachaturyan, Theory of Structural Transformations in Solids, Wiley & Sons, New York, 1983.

[11] V.V. Slezov, Kinetics of First Order Phase Transitions, Wiley-VCH, Weinheim, 2009.

[12] A. Onuki, H. Nishimori, Anomalously slow domain growth due to a modulus inhomogeneity in phase-separating alloys, Phys. Rev. B 43 (1991) 13649-13652.